Dependence of hydrocarbon sigma CC bond strength on bond angles: The concepts of "inverted", "direct" and "superdirect" bonds

Rubén Laplaza, Julia Contreras-García, Franck Fuster, François Volatron, Patrick Chaquin

Dependence of hydrocarbon sigma CC bond strength on bond angles: the concepts of "inverted", "direct" and "superdirect" bonds.

Rubén Laplaza,[b] Julia Contreras-Garcia[c], Franck Fuster [c], François Volatron[c], and Patrick Chaquin*[a]

Abstract. The bond energy (BE) of CC in CH_3-CH_3 with respect to geometry frozen fragments follows a sigmoidal increase as a function of the θ = HCC pyramidalization angle. Using dynamic orbital forces as a BE index, the same behaviour as a function of a unique <θ> parameter, mean angle of the substituents, is found for 24 single CC bonds in various hydrocarbons. Thus the <θ> parameter appears as a straightforward and robust index of the geometrical constraints which can either strengthen or weaken a bond. This way, CC sigma bonds can be easily classified into weak "inverted" bonds for <θ> < 90° (eg. in [111]propellane and bicyclobutane), "direct" (or "normal") bonds for 90° < <θ> < 120° (eg. ethane), and strong "superdirect" bonds for <θ> > 120° (eg. in tetrahedryl-tetrahedrane and butadiyne).

Keywords: Chemical bonding, Inverted bonds, superdirect bonds, orbital forces, hydrocarbons

Introduction

In a recent publication, we revisited the properties of the so-called "inverted bond" in [1.1.1]propellane (Figure 1)[1]. Let us recall that inverted bonds result from the overlap of s+p hybrids by their smaller lobe (Figure 1), by contrast to "normal" or "direct" bonds in which overlap occurs between their bigger lobes. The energy of the central CC bond of

[a] Pr. P. Chaquin
Laboratoire de Chimie Théorique (LCT)
Sorbonne Université, CNRS, F-75005 Paris
E-mail : chaquin@lct.jussieu.fr
[b] Dr. R. Laplaza
Laboratoire de Chimie Théorique (LCT)
Sorbonne Université, CNRS, F-75005 Paris

Departamento de Química Física
Universidad de Zaragoza
50009 Zaragoza, Spain
[c] Dr. J. Contreras-Garcia, Dr. F. Fuster, Dr. F. Volatron
Laboratoire de Chimie Théorique (LCT)
Sorbonne Université, CNRS, F-75005 Paris

propellane was evaluated [2] to ca. 60 kcal/mol and this unexpected high value was the subject of many works [3]. Its origin was attributed either to a strong σ bond of "charge shift" nature [3b] or to π-type three-electron two centers ensured by the CH_2 bridges [3c].

In ref [1], we used C_2H_6 models to mimic *in silico* the CC bond inversion by decreasing the θ = HCC angle from its optimized value, close to 111°, down to 70°. The CC dissociation energy, computed with respect to geometry frozen CH_3 moieties, was found to decrease rapidly and by extrapolation should tend to zero for HCC = 60°. The use Dynamic Orbital Forces (DOF) as indices of bond strengths confirmed this result: the intrinsic σ bond energy in propellane should be near zero, and thus the CC bonding is essentially π in nature. In a response by Braïda et al. [4], this result was contested, arguing that, due to its charge shift nature, the bond strength in propellane could not be evaluated using DOFs.

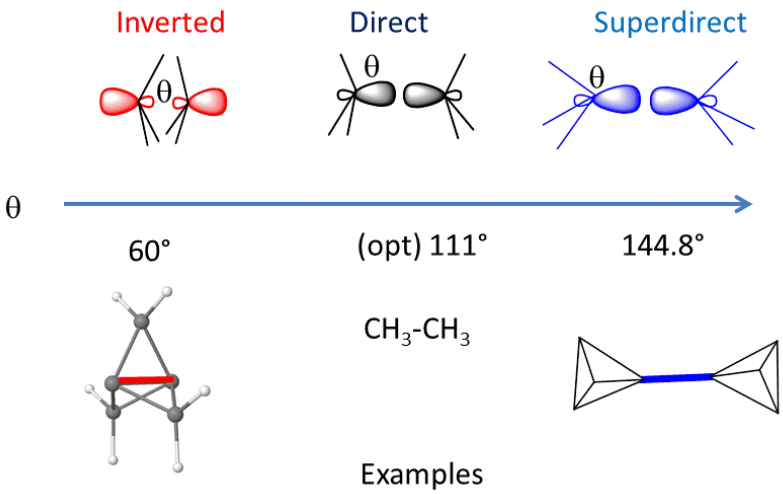

Figure 1. "Inverted", "direct" and "superdirect" bonds according to the θ angle of substituents. [1.1.1]Propellane, ethane and tetrahedryl-tetrahedrane exemplify these three types of bonds respectively.

By contrast, in some C-C bonds, the substituent angles are significantly greater than their value in ethane, with an associated increase of the bond energy. Though the unsubstituted molecule is unstable [5], tetrahedryl-tetraedrane (Figure 1) is the limiting example of such a situation, with substituent angles close to 145° and a central bond remarkably strong (136 kcal/mol) and short (1.426 Å) [6]. We propose the term "superdirect" for such bonds. Thus, as displayed in Figure 1, sigma bonds can be classified into "inverted", "direct" and "superdirect" according to the value of the θ pyramidalization angle.

In the present work, our aim is to study the dependence of σ CC bond strength of hydrocarbons on the bond angles of its substituents. In a first step C_2H_6 and related models will offer an *in silico* overview of this relation. Then, we will show that that the σ CC bond strength in any hydrocarbon can be characterized by a unique angle parameter leading to the concepts of "inverted", "direct" and "superdirect" bonds. For this purpose, bond strengths were compared using the Dynamic Orbital Forces (DOF) as indices of intrinsic bond energy and as a tool of σ/π partition in a panel of 35 bonds in 28 molecules.

Computational Details

Optimized geometries and bonding energies (BE) with respect to geometry frozen fragments have been calculated at the CCSD(T)/cc-pVQZ level for C_2H_6 and CH_3-H models, and at the MP2/cc-pVTZ level for Si_2H_6, Ge_2H_6 and N_2H_4. The geometry of 28 hydrocarbon molecules was also optimized at the MP2/cc-pVTZ level (see supplementary data). The derivatives of the canonical molecular orbitals were calculated, with the same basis set as geometry optimization, by a finite difference of bond lengths of 0.002 Å to 0.004 Å according to the case, thanks to a home-made script (available upon request). The Gaussian09 program was used throughout this work [7].

Results and discussion

1. *In silico* C_2H_6 and related models

1.1. Influence of HCC angles on CC bond energy in C_2H_6

In the C_2H_6 model, all six θ = HCC angles are frozen from 70° to 145°. After optimization of the remaining geometrical parameters, the C-C bond energy (BE) with respect to geometry frozen CH_3 moieties has been computed at the CCSD(T)/cc-pVQZ level. In this model (Table 1 and Figure 2), BE decreases rapidly when θ decreases from the optimized geometry to yield an inverted bond. It increases significantly when θ increases to yield a superdirect bond. The direct/superdirect limit has been taken somewhat arbitrarily for θ = 120°.

Table 1. The C_2H_6 model. Geometrical parameters R(Å) and bonding energy BE (kcal/mol, with respect to two CH_3 at frozen geometry) as function of θ (CCSD(T)/cc-pvQZ). The results for θ ≤ 111.2° are taken from ref. 1.

	C_2H_6									
θ	145°	140°	130°	120°	opt (111.2°)	100°	95°	90°	80°	70°
R(CC)	1.411	1.422	1.448	1.483	1.527	1.628	1.708	1.830	2.231	2.9
R(CH)	1.18	1.135	1.111	1.097	1.091	1.085	1.082	1.079	1.079	1.089
BE	154.2	152.8	145.0	131.6	114.1	81.6	63.3	44.5	15.4	5.6

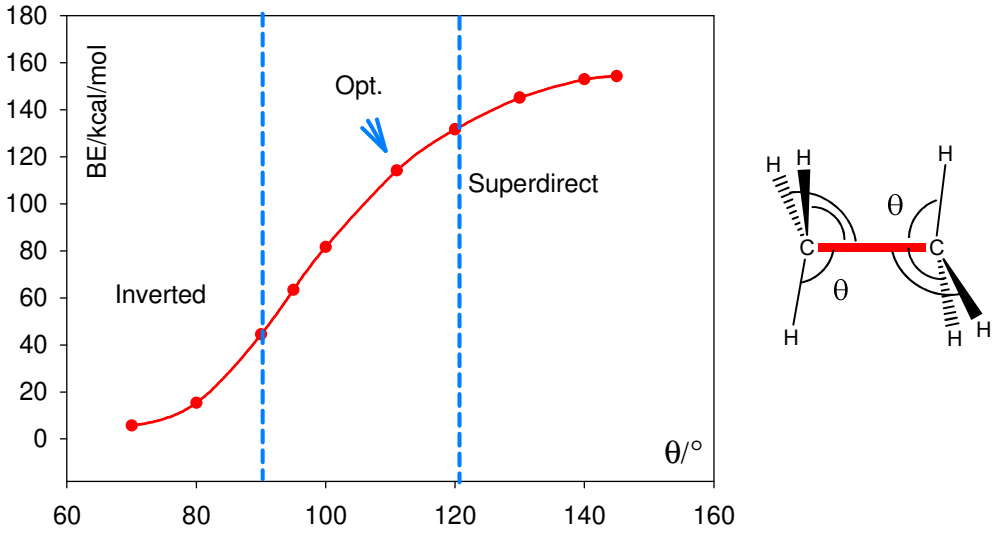

Figure 2. CC bond energy (BE) in C_2H_6 with respect to geometry frozen CH_3 fragments as a function of θ = HCC angles (θ = 111.2° optimized value); CCSD(T)/cc-pvQZ.

1.2. Qualitative interpretation

The overall sigmoidal shape of BE curve as a function of θ can be interpreted qualitatively by an evaluation of the overlap of both s+p hybrids, h_1 and h_2 (Figure 3).

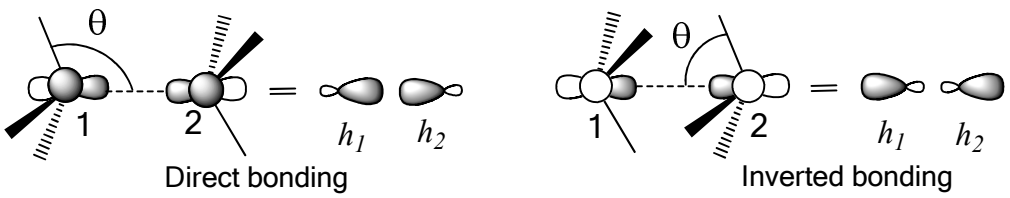

Figure 3. Overlap in direct and inverted bonding.

The hybrids h_1 and h_2 are written as:

$$h_1 = \alpha s_1 + \beta p_1$$
$$h_2 = \alpha s_2 + \beta p_2$$

with $\alpha^2 + \beta^2 = 1$. Setting $\beta > 0$:

$\alpha < 0$ for $\theta < 90°$

$\alpha = 0$ for $\theta = 90°$

$\alpha > 0$ for $\theta > 90°$

The theoretical limits of θ are 0°, with $\alpha = -\beta = -1/\sqrt{2}$ and 180°, with $\alpha = \beta = 1/\sqrt{2}$. The corresponding hybridization states can be referred to as sp^{-1} and sp respectively. Between these limits, the following hybridization states are encountered: sp^{-2} ($\alpha = -1/\sqrt{3}$), sp^{-3} ($\alpha = -1/2$), s^0p ($\alpha = 0$), sp^3 ($\alpha = 1/2$), sp^2 ($\alpha = 1/\sqrt{3}$). The following values of α for CH_3 are obtained with the minimal basis STO-3G for CH_3 and various θ (Table 2). For $\theta = 120°$, the calculated s participation to the hybrid is found 0.6, close to ½ which is the theoretical value for sp^2. This angle value can be taken as the (arbitrary) limit between "direct" and "superdirect" bonds.

Table 2. Coefficient α of the s AO in the CH_3 SOMO hybrid as a function of θ angle (see Figure 3).

θ	**60°**	**70°**	**80°**	**90°**	**100°**	**110°**	**120°**	**130°**	**140°**
α	-0.601	-0.483	-0.294	0.000	0.294	0.483	0.601	0.693	0.786

The overlap *S* of h_1 and h_2 is given by:

$$S = \langle \alpha s_1 + \beta p_1 | \alpha s_2 + \beta p_2 \rangle = \alpha^2 \langle s_1 | s_2 \rangle + \beta^2 \langle p_1 | p_2 \rangle + 2\alpha\beta \langle s_1 | p_2 \rangle \qquad (1)$$

In a first step, the overlaps S_{eq} of s+p hybrids of CH_3 have been computed at the CC equilibrium distances in the C_2H_6 model for each θ value (red curve in Figure 4a). Then, in order to emphasize the effect of hybridization alone, the overlap S_0 has been determined for a constant CC distance of 1.5 Å. Note that, in this case, to a first approximation, the three atomic overlaps in Eq. 1 are close to 0.3:

$$S_0 \approx 0.3(\alpha^2 + \beta^2 + 2\alpha\beta) = 0.3(1 + 2\alpha\beta) \qquad (2)$$

The corresponding values are reported in Figure 4a (black curve). Both S_0 and S_{eq} as a function of θ have a sigmoidal shape similar to the bonding energy in Figure 2. The two curves are nearly coincident for $\theta < 110°$ indicating the prominent role of the hybridization in

this region. Moreover, the bonding energy appears closely connected to both S_{eq} *and* S_0 (Figure 4 (b)), with, again a quasi-superimposition in the corresponding region.

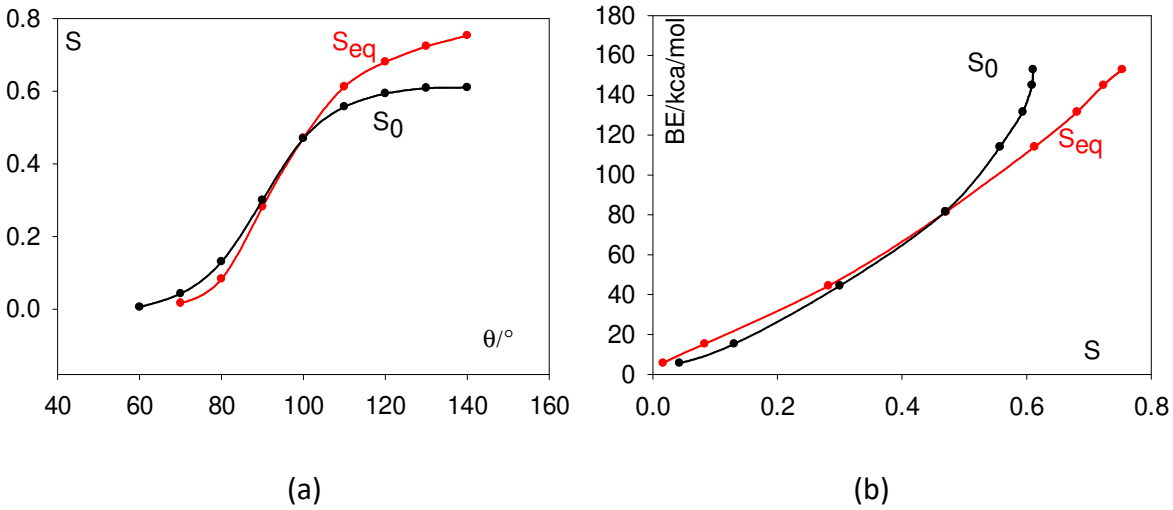

Figure 4. (a) Variation of overlap S with θ in C_2H_6 model: S_{eq} at equilibrium R(CC) distance (red curve); S_0 for a CC constant distance of 1.5 Å (black curve). (b) Variation of CC bond energy BE as a function of S_{eq} (red curve) and S_0 (black curve).

Finally, this model emphasizes the role on BE of the overlap of the two s+p hybrids which increases with θ, together with α, algebraic participation of the s AO to these hybrids.

1.3. Related models: Si_2H_6, Ge_2H_6, N_2H_4 and CH_4

Though we are mainly interested in CC bonds in this work, we examined some models involving other bonds to compare their behaviour when similar angle constraints are imposed.

Two heavier systems, Si_2H_6 and Ge_2H_6, have been studied at the MP2/cc-pVTZ level following the approach of the C_2H_6 model. Figures 5(a) and 5(b) display the variation of BE as a function of the θ angles H-Si-Si and H-Ge-Ge respectively. The two curves are very similar. They have also the same general shape as for C_2H_6, with a weaker BE increase in the superdirect region (θ > 120°). It appears that the decrease of the ns-np gap in these both species, with respect to C_2H_6, is only of minor consequence as compared to the angle variation.

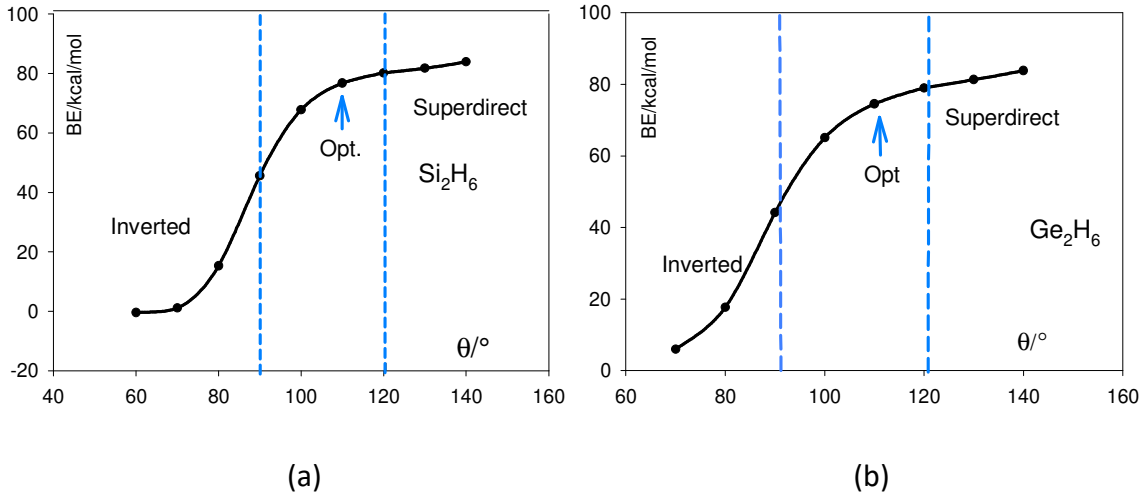

Figure 5. Central bond energies (BE) of Si_2H_6 (a) and Ge_2H_6 (b) with respect to geometry frozen AH_3 fragments as functions of θ angles H-Si-Si and H-Ge-Ge respectively (MP2/cc-pVTZ).

The BE of the NN bond of NH_2-NH_2 in D_{2d} symmetry was also studied as a function of θ = HNN angles. The dissociation energy was computed with respect to geometry frozen NH_2 fragments in their $^2A_1$ state. It should be noted that N-N bond breaking results in the formation of two NH_2 radicals possessing a lone pair in a 2p AO and a semi occupied s+p hybrid. In its optimized geometry, this state is ca. 34 kcal/mol above the $^2B_1$ ground state [8]. Thus the value of BE in geometry optimized N_2H_4 lies at 68 kcal/mol above the NN dissociation energy into $2NH_2$ in their ground state.

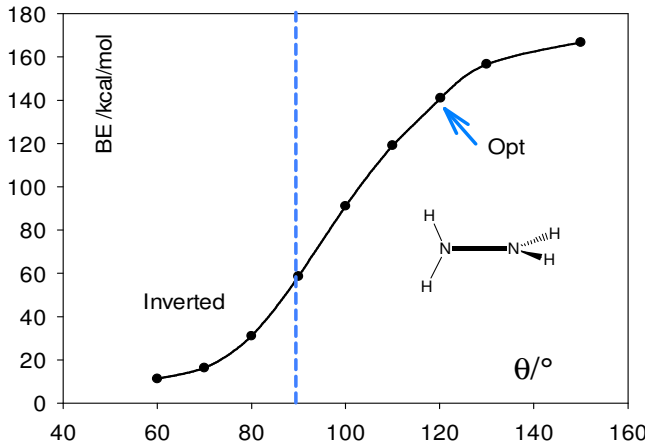

Figure 6. N-N bond energy (BE) in N_2H_4 (D_{2d}) with respect to geometry frozen NH_2 fragments as a function of θ = H-N-N angles (MP2/cc-PVTZ).

Finally, we studied the energy of one C-H bond in CH_4 as a function of the θ pyramidalization angle of the CH_3 moiety. Results in Table 3 and Figure 6 are similar to the preceding ones. Nevertheless, because we deal here with the deformation of only one CH_3 group, yielding either "semi-inverted" or "semi-superdirect" bonds, the relative variation of BE is smaller than in the case of C_2H_6 (cf. Figure 2). Note that the influence of bond angles on bond lengths has already been studied in CH_4 and related species [9].

Table 3. H_3C-H. Geometrical parameters R (Å) and bond energy BE of CH (kcal/mol, with respect to H and CH_3 at frozen geometry) as function of θ; opt = 109.5°; CH1 refers to H in CH_3 group; CCSD(T)/cc-pVQZ level of calculation.

	H_3C-H								
θ	140°	130°	120°	opt	100°	90°	80°	70°	60°
R(CH)	1.063	1.068	1.076	1.087	1.105	1.132	1.174	1.229	1.290
R(CH1)	1.134	1.108	1.095	1.087	1.085	1.084	0.876	1.003	1.130
BE	138.4	134.1	127.7	119.4	107.5	90.6	70.8	54.1	44.9

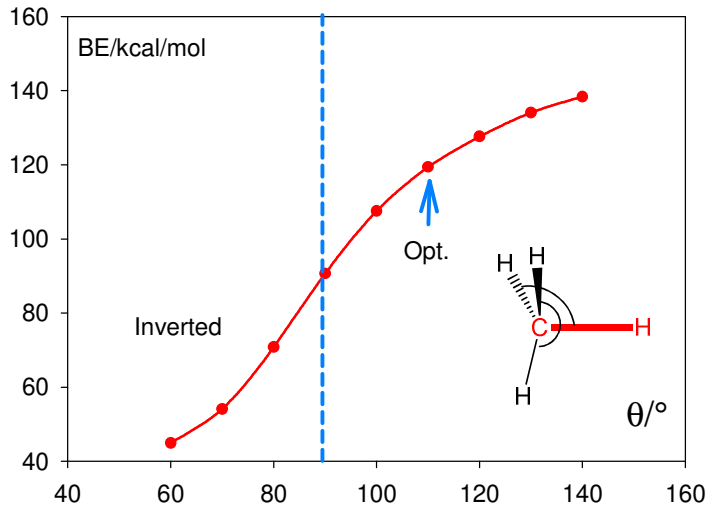

Figure 7. CH bond energy (BE) in H_3C-H (red bond) with respect to H and geometry frozen CH_3 fragments as a function of θ = HCH angle (CCSD(T)/cc-pvQZ).

All studied models agree with the fact that the bond energy is strongly dependent on the substituent angles: it decreases rapidly with the inverted character of the bond and increases with its superdirect character. These phenomena follow the same variation as C_2H_6 in section 1.1 which suggest that they can be interpreted similarly by of the hybridization of the s+p AOs overlapping in the bond formation, controlled by these angles. Specifically, BE increases with the s (algebraic) coefficient in the s+p hybrids. This result is well-known for "direct" C-H bonds with aliphatic (sp^3), ethylenic (sp^2) and acetylenic (sp) carbons as well as

in direct C-C bonds [10], for example regarding the strong central bond of tetrahedryl-tetraedrane [6b,11]. Nevertheless, the final optimized CC distance involves other parameters as evidenced by energy decomposition analysis [12]. Moreover, it was shown in a recent work that the contraction of CC bonds along a series $C(sp^3)$-$C(sp^3)$, $C(sp^3)$-$C(sp^2)$ and $C(sp^3)$-C(sp) does not originate from an increase in the s character of the second atom, but in a decrease of the steric (Fermi) repulsion between substituents of both carbons [13]. Indeed, in the AH_n-AH_n models of the preceding study, we observe that direct bonds shorten as θ increases, together with H…H distances resulting in weaker Fermi repulsion. The situation is less clear for inverted bonds. As an example, in C_2H_6, for θ = 90° R(CC) = 1.830 Å with H…H = 2.12 Å. For θ = 80° the H…H distance increases very weakly (2.14 Å), resulting in a negligible decrease in Fermi repulsion, while R(CC) significantly increases by 0.4 Å (2.231 Å). It suggests that the bond length could be controlled by hybridization in inverted bonds.

2. Inverted, direct, and superdirect bonds: generalization for sigma CC bonds in hydrocarbons

2.1. Mean angle <θ> of substitution

The preceding models preserve a symmetry axis along the bond under scrutiny with equal pyramidalization angles of H substituents on each heavy atom. We will now extend the inverted/direct/superdirect character to any CC σ bond in hydrocarbons, be it formally a single bond or a σ bond in a formally multiple bond. For this purpose, we define a <θ> parameter as simply the mean value of the angles of the six substituents on both carbon atoms; the π bonds are treated as σ ones in these calculations. Two examples are given in Figure 8.

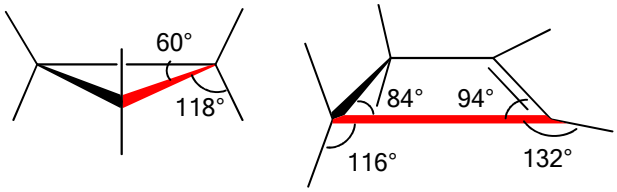

Figure 8. Calculation of the <θ> angle for the red bond in cyclopropane and cyclobutene.

In cyclopropane, the red bond has 4 H at 118° and two C at 60°, yielding <θ>≈ 99°. In cyclobutene, the red bond is considered as having 2 C at 94°, 1 H at 132°, 1 C at 84° and 2H at 116.° yielding <θ> = 106°. This way, the central C-C bond in butadiyne HC≡C—C≡CH has the <θ> theoretical maximum value of 180°. In formally multiple bonds, the <θ> angle is determined in a similar way. For example, in acetylene H-C≡C-H, the σ CC bond in considered as having 4 C at 0° and 2 H at 180°, yielding <θ> = 60°.

2.2. Dynamic orbital forces as index of intrinsic bond energy and tool for σ/π partition

For the study of the relation between σ bond strength and <θ> in real systems, 35 CC bonds of various <θ> were considered in a panel of 28 molecules (Tables 4 and 5). In many of these cases, the BE of C-C bonds can no longer be computed in the same way as in the first section, namely by dissociation of two geometry frozen fragments. Thus we will use the dynamic orbital forces (DOF)[14] as indices of bond energies.

According to Koopman's theorem, the derivative of the i^{th} canonical MO energy ε_i with respect to a bond length (R(CC) in the case of a CC bond) is:

$$\frac{d\varepsilon_i}{dR(CC)} = \frac{dE^0}{dR(CC)} - \frac{dE_i^+}{dR(CC)} \qquad (3)$$

where E_0 is the energy of the neutral species and E_i^+ the energy of the ion resulting from the loss of one electron in the i^{th} MO. This relation is exact if the MOs are the same for the neutral and cationic species (frozen MO approximation). If the geometry of the neutral species is optimized, $dE^0/dR(CC) = 0$ and the DOF is thus the opposite of the force exerted along R(CC) upon diabatic ionization. It has already been used as a measure of the bonding/antibonding character of the MO with respect to this bond [15]. Also it has been shown that a MO of positive DOF has a positive contribution to the dissociation energy and vice-versa [16]. Thus one can assume that the sum Σ_{tot} of these derivatives over valence MOs occupied by n_i electrons :

$$\Sigma_{tot} = \sum_i^{occ} n_i \frac{d\varepsilon_i}{dR(CC)}$$

is an index of bond strength. This idea has been successfully developed [1, 17, 18], especially in the case of CC bond in hydrocarbons [1, 18]. Also, this quantity can be decomposed into σ (Σ_σ) and π (Σ_π) components allowing to compare these both contributions:

$$\Sigma_{tot} = \sum_i^{occ} n_i \frac{d\varepsilon_i}{dR(CC)} = \sum_j^{\sigma occ} n_j \frac{d\varepsilon_j}{dR(CC)} + \sum_k^{\pi occ} n_k \frac{d\varepsilon_k}{dR(CC)} = \Sigma_\sigma + \Sigma_\pi$$

However Σ_{tot} is an intrinsic quantity of the system, whereas the bond energy dissociation with respect to geometry frozen fragments (BE) considered in section 1 involves the electronic relaxation of fragments and thus some reorganization energy. This tends to lower BE with respect to the intrinsic bond energy, but this difference should be small if the two following conditions are fulfilled: (i) the bond is symmetrically or nearly symmetrically substituted, resulting in a negligible electron transfer by bond dissociation and (ii) no significant stabilization of the radicals obtained occurs by conjugation or hyperconjugation. In Figure 9, we report BE as a function of Σ_{tot} for the C_2H_6 model and various CC bonds (taken from ref. 18). We observe an excellent linear correlation (R^2 = 0.98) of BE of CC bonds and Σ_{tot} in the series C_2H_2, C_2H_4, C_6H_6, C_2H_6 and C_3H_6 (black line in Figure 9). Regarding the C_2H_6 model with various θ values (red curve in Figure 9), the curve is strictly superimposed to the preceding black line for Σ_{tot} > 0.4. For smaller Σ_{tot} values, the slope decreases and BE tends to zero for Σ_{tot} ≈ 0.

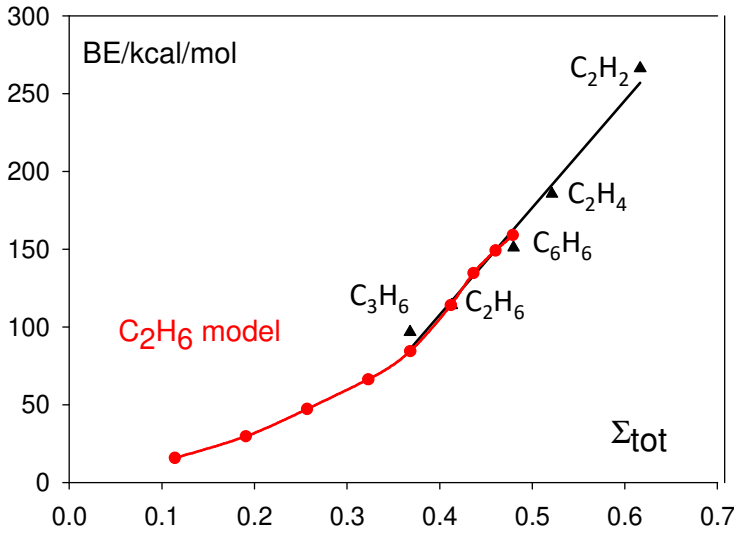

Figure 9. Bond energy (kcal/mol) with respect to geometry frozen fragments (MP2/cc-pVTZ) as a function of Σ_{tot} (a.u.).

This way, Σ_{tot}, though computed from H-F level MOs, is found to be correlated to CC bond strength. This result is empirical, but further supported by a large amount of evidence regarding bond energies. Indeed, a very good correlation (R^2 = 0.97) is found with respect to BE values calculated at the DFT ωB97XD/aug-qzvp level for bonds **1, 12**, **19**, **27, 26, 29, 34** of Tables 4 and 5 [19]. Moreover, Σ_{tot} can be compared with intrinsic bond energies computed from AIM critical point properties and bond paths (using, of course, correlated electron densities) [20]: a good linear correlation is again obtained (R^2 = 0.96) with the set of bonds **1**, **4**, **8**, **9**, **12**, **13**, **18**, **19**, **26**, **29**, **30**, **33, 34** of Tables 4 and 5 (see Supplementary data Fig. 1). Clearly, the fact that electron correlation is not included in Σ_{tot} can be questionable. Nevertheless, KS MOs obey eq. 3 only approximately, with discrepancies depending on the nature of the functional [21]. Moreover, a lower correlation of the CC BEs of the five molecules of Fig. 9 is observed with Σ_{tot} from KS MOs of various functionals: R^2 = 0.92 (B2PLYP), 0.92 (CAM-B3PLYP), 0.74 (B3LYP) respectively, vs. 0.98 (H-F). Thus, as far as the molecule is satisfactorily described at the H-F level, we can consider Σ_{tot} as a straightforward *empirical* index allowing the comparison of the CC intrinsic bond strengths in hydrocarbons, with a decomposition into Σ_{σ} and Σ_{π} reflecting their relative σ and π components.

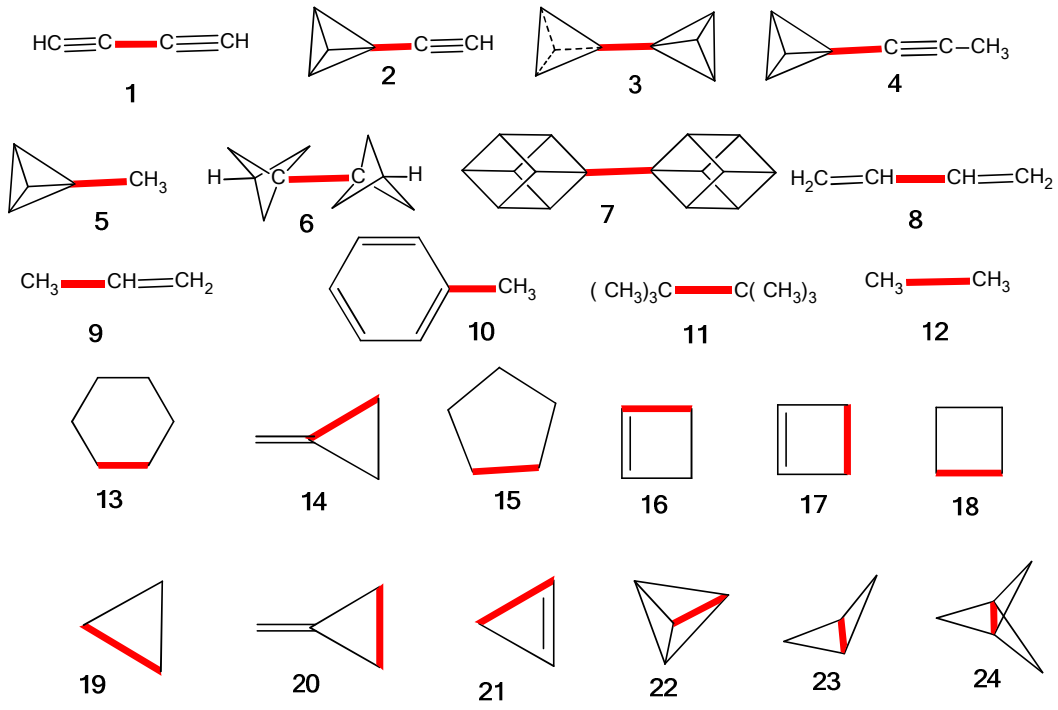

Figure 10. Bonds (red bold) and molecules of Table 4.

2.3. Sigma CC bond energy and mean angle of substitution <θ>

2.3.1. Formally single bonds

In Table 4, we report the values of Σ_{tot}, Σ_{σ} and Σ_{π} in a panel of formally single 24 C-C bonds, displayed in Figure 10, by order of decreasing values of <θ> from 180° to 60°. The concept of directedness/invertedness concerns σ bonds, and thus we will be interested mainly in the Σ_{σ} component, though Σ_{tot} and Σ_{π} could also offer useful information.

Table 4. Values of Σ_{tot} , Σ_{σ}, Σ_{π} (a.u.); % of Σ_{π} in Σ_{tot} , equilibrium bond length R(CC) (Å) and the corresponding values of <θ> (°) for formally single C-C bonds (TET = tetrahedryl; BCP = bicyclopentyl; CUB = cubyl, see also Figure 10).

Label	Molecule	Σ_{tot}	Σ_{σ}	Σ_{π}	% π	R(CC)	<θ>
1	HC≡C—C≡CH	0.513	0.450	0.064	12.4	1.369	180
2	TET—C≡CH	0.527	0.437	0.090	17.1	1.394	163
3	TET—TET	0.468	0.447	0.021	4.5	1.419	145
4	CH_3—C≡CH	0.458	0.415	0.042	9.1	1.458	145
5	TET—CH_3	0.495	0.442	0.053	10.1	1.476	128
6	BCP—BCP	0.489	0.434	0.055	11.3	1.477	127
7	CUB—CUB	0.478	0.420	0.058	12.1	1.465	125
8	CH_2=CH—CH=CH_2	0.478	0.433	0.045	9.4	1.453	121
9	CH_3—CH=CH_2	0.418	0.399	0.019	4.5	1.505	116
10	Ph—CH_3	0.415	0.397	0.019	4.6	1.503	115
11	$(CH_3)_3C$—$C(CH_3)_3$	0.439	0.392	0.048	10.8	1.565	111
12	CH_3—CH_3	0.413	0.392	0.021	4.9	1.527	111
13	cyclohexane	0.445	0.425[a]	0.02[a]	4.5[a]	1.565	110
14	methenecyclopropane (3-4)	0.414	0.397	0.017	4.1	1.464	109
15	cyclopentane	0.420	0.403	0.017[b]	4.3	1.526	108
16	cyclobutene (2-3)	0.445	0.400	0.045	10.1	1.537	106
17	cyclobutene (3-4)	0.404	0.396	0.008	2.0	1.565	105
18	cyclobutane	0.408	0.401	0.007[b]	1.7	1.546	105
19	cyclopropane	0.364	0.368	-0.004	-1.1	1.504	99
20	methenecyclopropane (1-2)	0.333	0.333	0.000	0.0	1.539	97
21	cyclopropene	0.281	0.283	-0.002	-2.0	1.508	88
22	tetrahedrane	0.353	0.278	0.075	21.2	1.478	88
23	bicyclobutane	0.360	0.215	0.146	39.7	1.500	82
24	[1.1.1]Propellane	0.275	-0.029	0.304	110.5	1.596	60

[a] Estimated on the basis of the same Σ_{π} =0.02 a.u. as **12**. [b] The π MOs have been visually identified, which can lead to some uncertainty.

Molecules **1**-**8** can be considered as having a superdirect bond, with Σ_σ ranging from 0.415 up to 0.450 a.u. for butadiyne **1,** which has the maximum theoretical value of <θ> (180°). For the direct bonds **9**-**18 (**116° **<** <θ> < 105°) **,** Σ_σ is generally close to 0.4 a.u. Ethane **12** can be taken as the prototype of "standard" direct CC bond with Σ_σ = 0.392 a.u. Bonds **19** and **20**, are formally direct (<θ> = 99° and 97° respectively) but have significantly lower Σ_σ (0.368 and 0.333 a.u. respectively) according to ring strain. Molecules **21**-**24** possess inverted bonds and Σ_σ less than 0.283 a.u., corresponding to strong strains, down to a slightly negative value in propellane **24** (-0.029 a.u. with <θ> = 60°).

We thus observe (Figure 11) a general increase of Σ_σ with <θ>, following the same sigmoidal shape as observed for the models of sections 1 and 3. As a landmark, we report on the same figure the variation of Σ_σ for the C_2H_6 model (red curve), showing that the behaviour of real bonds is quite similar to that of this C_2H_6 model.

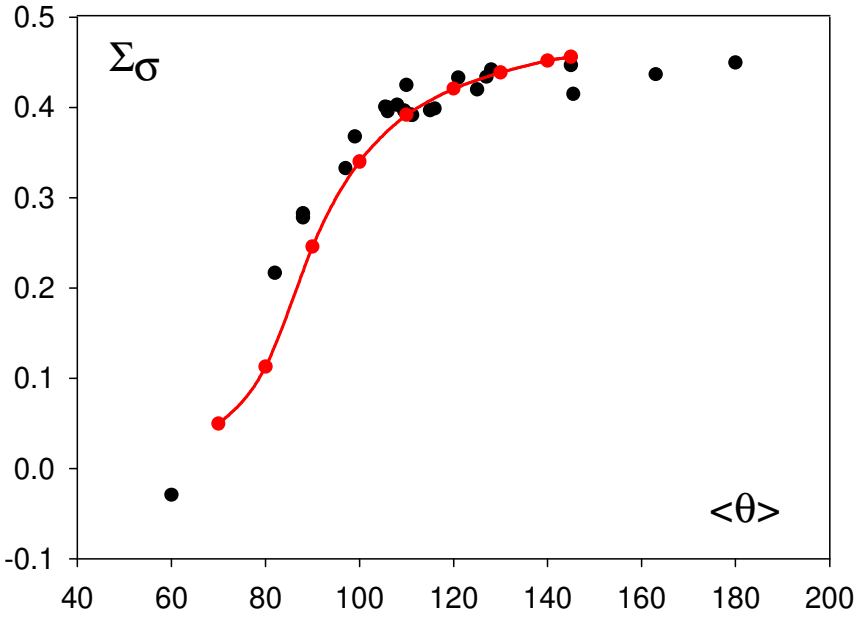

Figure 11. Σ_σ (a.u.) values for bonds in molecules **1**-**22** with respect to the mean substituent angle <θ> (°). The red curve corresponds to C_2H_6 model.

The value of Σ_{tot} in tetramethylbutane **11** (0.439 a.u.) suggests that its intrinsic bond energy is greater than that of ethane **12** (0.413 a.u.) though its experimental dissociation energy is significantly smaller (78.6 kcal/mol vs. 90.2 kcal/mol) [22]. Nevertheless, the BE of both

species with respect to geometry frozen fragments (MP2/cc-PVTZ) are found nearly equal (113.0 kcal/mol for **11** and 113.9 for **12**). Moreover, the electronic relaxation in $Me_3C^{\cdot}$ radical involves a significant stabilization by hyperconjugation, which leads to an underestimation of the calculated BE of **12** with respect to the actual intrinsic bond strength.

The π participation to Σ_{tot}, corresponding to the total bond strength, is generally no more than ca. 10 % in all superdirect or direct bonds. In can be noted that the high BE in butadiyne **1** as compared to that of ethane **12** is due to σ strengthening ($\Delta\Sigma_\sigma$ = 0.058 a.u.) more than to conjugation ($\Delta\Sigma_\pi$ = 0.043 a.u.). The same remark holds for butadiene **8**, whose corresponding values are $\Delta\Sigma_\sigma$ = 0.041 a.u. and $\Delta\Sigma_\pi$ = 0.024 a.u. Also, it has been proposed that the strong bond of **3** originates equally both from its high s character and from hyperconjugation [23]; but in the present work the hyperconjugation term appears weak, with only 4.5 % contribution of π MOs to Σ_{tot}. This is further supported by the 12% of π energy that was determined from Energy Decomposition Analysis [6b].

In the series of cyclanes, we observe a regular decrease of Σ_{tot}, as the ring strain increases: cyclohexane **13** (0.445 a.u.), cyclopentane **15** (0.420 a.u.), cyclobutane **18** (0.408 a.u.) and cyclopropane **19** (0.368 a.u.). Because their rings are non-planar (except cyclopropane **19**), the π MOs have been identified visually for **15** and **18**. For cyclohexane **13** the σ/π partition becomes problematic because most of the MOs have both types of participation; we assumed that Σ_π is close to the value observed for ethane. Under these conditions, a decrease of Σ_σ is also observed along the series together with $\langle\theta\rangle$. The slightly negative π participation in **19** and **21** can be due to their quasi-eclipsed conformation, this participation being nearly zero in eclipsed ethane. Furthermore, it is well known that cyclobutane **18** and cyclopropane **19** have very close strain energies, 26.5 kcal/mol and 27.5 kcal/mol respectively [24], though the three-membered cycle could appears as much more strained. Taking into account that these energies involve all the bonds, it has been suggested that three weaker CC bonds in cyclopropane are compensated by six stronger CH bonds [25]. Indeed, $\langle\theta\rangle$(CH) = 109.5° for **18** and 116.3° for **19**: thus the CH bonds in cyclopropane are found to have some superdirect character. Moreover, from Table 3, the C-H BE increase can be evaluated to ca. 6.9 kcal/mol, close to previous determinations (8.6-8.8 kcal/mol) [26].

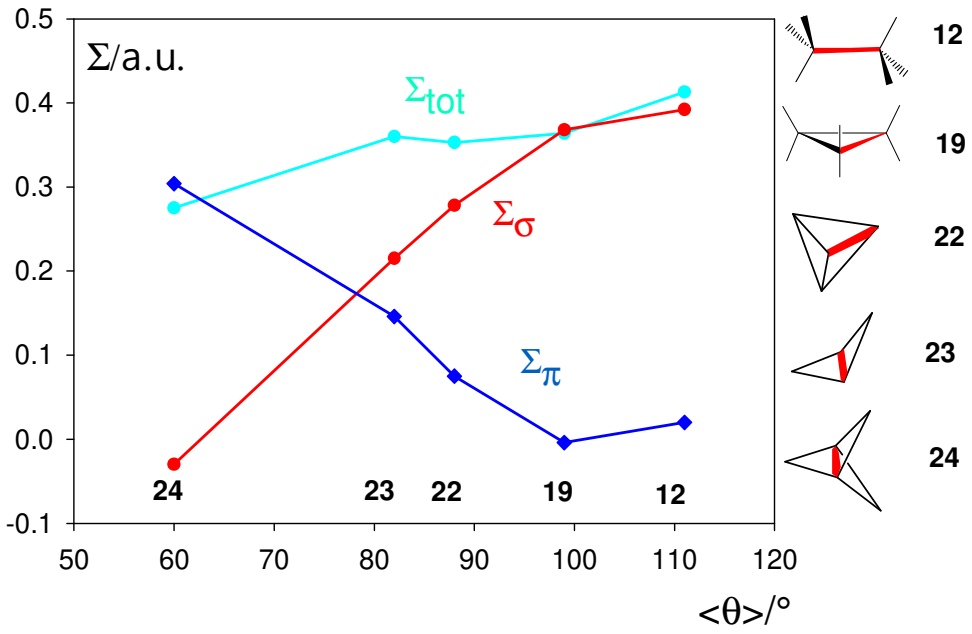

Figure 12. Various Σ values (a.u.) for CC bonds in ethane and a series of three-membered cyclic molecules (red bond).

The series of three-membered ring species **19**, **22**, **23** and **24**, compared to ethane **12** (Figure 12), is of a particular interest. The CC bond undergoes a progressive inversion with <θ> decreasing from 111.2° (direct bond in **12**) to 60° (inverted bond in propellane **24**). Σ_σ decreases monotonously from 0.392 a.u. in ethane down to -0.029 a.u. in propellane. But at the same time, this decrease is compensated to a large extent by an increase of Σ_π for **22**, **23** and **24**. As a matter of fact, the presence of two CH bridges in **22**, two and three CH_2 bridges in **23** and **24** respectively, allows the formation of three-center two-electron bonds of π character. The relative contributions of MOs to σ and π bonding have been detailed in ref. [1] in the case of propellane **24**. The "CH_2 bridge" MOs of bicyclobutane **23** are displayed in Figure 13, together with their respective DOF. They are characterized, according to their π nature, by a nodal plane containing the central bond and are of a_2 and b_2 symmetry within the C_{2v} group. One of these MOs (14) is found antibonding (DOF = -0.069 a.u.) while the other three are bonding. It is worthy to insist on the fact that, on the basis of the evolution of the Σ and <θ> values, the central bond of propellane **24** behaves as expected in this series and does not appear as a particular case, in spite of its "charge shift" character within VB method [3b].

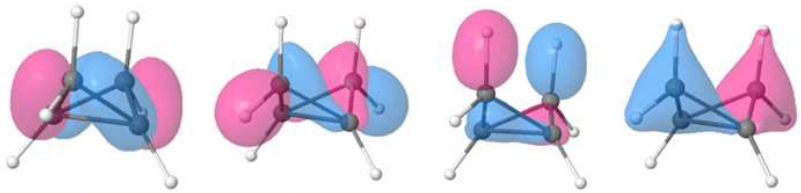

MO	14	12	10	6
Symmetry	a_2	b_2	b_2	b_2
DOF	-0.069	0.061	0.049	0.033

Figure 13. Bridge bond MOs, and corresponding DOF (a.u.) of bicyclobutane **23**.

The variation of R(CC) as a function of <θ> deserves a comment. Bonds **1-13** have generally a weak π participation and they are not subject to cycle constraints. Their lengths thus result from a free interplay of their strength (essentially controlled by their s component) and the Fermi repulsion of their substituents: both these parameters tend to shorten the CC bond as <θ> increases, as observed in Figure 14 (blue squares). These bonds have the same characteristics as the CC bond in the C_2H_6 model which behaves similarly (red curve). By contrast, bonds **14**-**24** are subject to cycle constraints and π component of various importance, and their bond lengths (cyan circles) diverge from those of the C_2H_6 model.

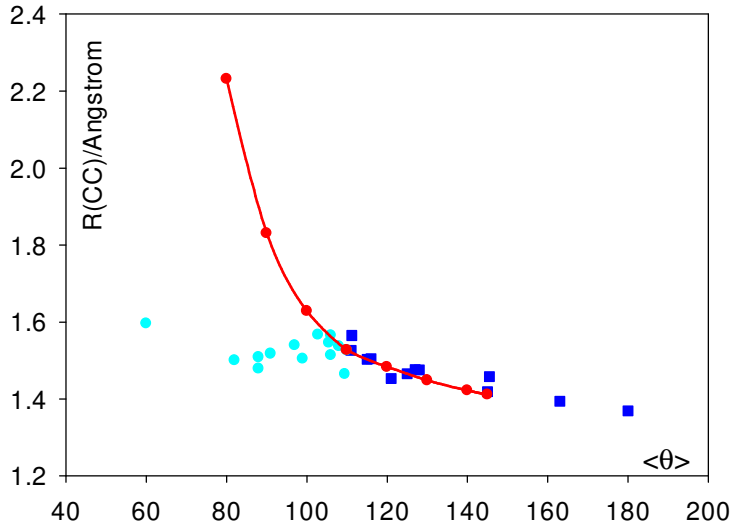

Figure 14. Bond lengths (Å) vs. mean angle <θ>; bonds **1**-**12** (blue squares); bonds **12**-**24** (cyan circles); C_2H_6 model (red curve).

2.3.2. Sigma bonds in formally multiple bonds

From a panel of 11 formally multiple bonds, displayed in Figure 15, we report in Table 5 the values of Σ_{tot} , Σ_{σ}, Σ_{π} (a.u.) and the mean angle <θ> calculated for their σ component. For benzene **24**, <θ> = 100° is the mean of the two values of Kékulé structures.

The Σ_{tot} values range from 0.479 a.u. to 0.579 a.u. for double bonds, from 0.577 a.u. to 0.616 a.u. for triple bonds and is 0.480 a.u. for the "half double bond" of benzene. As expected, Σ_{tot} is slightly smaller in the conjugated **30** and **33** than in the corresponding non conjugated **29** and **34**.

Table 5. Values of Σ_{tot}, Σ_{σ}, Σ_{π} (a.u.) for CC bonds in multiple bonds and the corresponding values of <θ> (°) for their σ bond (=C_3H_4 : cyclopropylidene, cf. Fig. 15).

label	Molecule	Σ_{tot}	Σ_{σ}	Σ_{π}	% π	R(CC)	< θ>
25	$H_2C{=}C{=}CH_2$	0.516	0.315	0.201	39.0	1.308	100
26	C_6H_6	0.480	0.342	0.139	29.9	1.394	100[a]
27	$H_4C_3{=}C_3H_4$	0.537	0.354	0.183	34.0	1.316	97
28	$CH_2{=}C_3H_4$	0.479	0.283	0.196	40.9	1.323	90
29	$H_2C{=}CH_2$	0.521	0.267	0.254	48.8	1.332	81
30	$CH_2{=}CH{-}CH{=}CH_2$	0.488	0.256	0.232	52.6	1.340	80
31	cyclobutene	0.519	0.283	0.236	45.5	1.350	77
32	cyclopropene	0.579	0.277	0.304	52.5	1.300	71.5
33	$HC{\equiv}C{-}C{\equiv}CH$	0.577	0.159	0.418	72.4	1.219	60
34	$HC{\equiv}CH$	0.616	0.145	0.471	76.5	1.211	60
35	cyclopentyne	0.524	0.087	0.437	83	1.245	40

[a] Mean value of the two Kékulé structures.

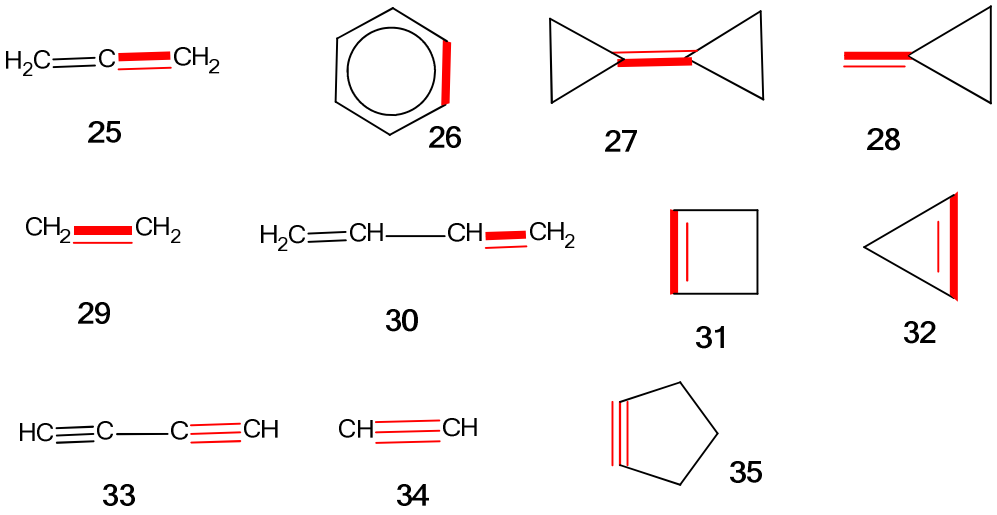

Figure 15. Bonds (red bold) and molecules of Table 5.

The <θ> values corresponding to the σ part of the double and triple bonds are greater than 90° only in **25**, **26** and **27.** Indeed, their Σ_σ values are smaller than that of cyclopropane **19** (0.372 a.u.). The σ participation to Σ_{tot} is generally close to 50% in standard alkenes and no more than ca. 25% in alkynes, which has been already noted [16]. Their variations as a function of <θ> are shown in Figure 16 with the same scale as in Figure 11 for the sake of comparison. Like in formally single bonds, Σ_σ tends to decrease with <θ>, but significantly more slowly. From these results, the σ bond in multiple bonds can be generally considered as formally inverted.

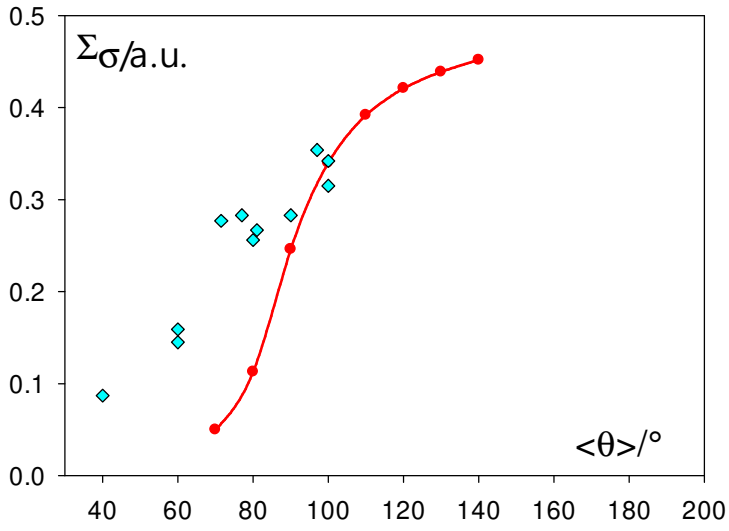

Figure 16. Values of Σ_σ (a.u.) for the σ bond in the formally multiple bond compounds **22**-**33** (cyan diamonds). The red curve corresponds to the C_2H_6 model for comparison.

The series **27**, **28** and **29** is illustrative of the influence of bond angles on σ bonds in double bonds (Table 5). The presence of two and one cyclopropenyl fragments in **27** and **28** respectively tends to increase <θ> and Σ_σ, with respect to **29**. The same evolution is observed from cyclobutene **31** to cyclopropene **32**.

The σ bonds of alkynes possess formally four C substituents at 0° and thus have a maximum <θ> value of 60°. Because cyclopropyne and cyclobutyne are unstable, cyclopentyne **35** appears to possess a σ bond with the smallest possible <θ> value (40°) and thus the weakest Σ_σ (0.087 a.u.) among all multiple bonds considered. In turn, the small <θ> value for σ in triple bonds entails for <θ>(CH) its maximum theoretical value of 180° in **33** and **34**, in agreement with high CH bond dissociation in acetylene and hydrogen cyanide.

Conclusion

The bonding energy BE of the CC bond in the CH_3 -CH_3 model is strongly dependant of the θ = HCC angles, exhibiting a sigmoidal variation. Starting from θ equilibrium value, BE decreases rapidly when θ decreases to yield “inverted bonds” (θ < 90°) and tends to zero for θ = 60°-70°. On the contrary, BE increases when θ increases above its equilibrium value. We propose the term “superdirect” for the latter type of bonds. Within MO framework, this general behaviour is closely related to the s participation in the s+p hybrid AOs involved in the CC bond.

These results are generalized to any CC sigma bond in hydrocarbons using the sum of dynamic orbital forces (DOF) as index of intrinsic bond energy. The strength of σ bonds is essentially controlled by a unique <θ> parameter, mean value of its substituent angles. In formally single CC bonds, this strength increases according to a sigmoidal variation as function of <θ> (from a panel of 24 bonds in 22 molecules). The difference of <θ> from the standard value of ca. 110° appears as a crude, but straightforward and robust, index of the strain exerted on a σ bond. For <θ> < 110° values, this strain is “negative” which weakens

the bond as its “inverted” character increases; for <θ> > 110° this strain is “positive”, resulting in a strengthening of the bond as its “superdirect” character increases.

As a matter of fact, the weakest sigma bonds are encountered in tetraedrane (<θ> = 88°), bicyclobutane (<θ> = 82°), vanishing in propellane (<θ> = 60°). At the opposite, the strongest σ CC bonds are found in butadiyne (<θ> = 180°) and bonds having tetrahedryl and/or ethynyl substituent(s) (<θ> >120°). It also accounts for the strain energy of cyclanes.

We also considered σ bonds in formally multiple bonds, with a panel of 11 molecules. These systems correspond to small <θ> values and σ bonds significantly weaker than in standard single bonds. This way, σ bonds in multiple bonds can be considered as formally inverted in most of cases.

[1]R. Laplaza, J. Contreras-Garcia, F. Fuster , F. Volatron, P. Chaquin, *Chem. Eur. J*. **2020**, *26*, 6839-6845.

[2] a) K. B. Wiberg, F. H. Walker, *J. Am. Ckem. Soc.* **1982,** *104,* 5239-5240; b) D. Feller, E. R. Davidson, *J. Am. Chem. Soc.* **1987***, 109,* 4133-4139; c) J. E. Jackson, L. C. Allen, *J. Am. Chem. Soc* **1984**, *106*, 591-599.

[3] a) T. Kar, K. Jug, *Chem. Phys. Lett*. **1996**, *256*, 201-206; b) W. Wu, J. Gu, J. Song, S. Shaik, P. C. Hiberty *Angew. Chem*. **2009**, *121*, 1435 –1438; c) M. D. Newton, J. M. Schulman, *J. Am. Chem. Soc*. **1972**, *94*, 773-778; d) W. Stohrer, R. Hoffmann, *J. Am. Chem. Soc.* **1972***, 94,* 779-786; e) E. Honegger, H. Huber, E. Heilbronner, *J. Am. Chem. Soc*. **1985**, *107,* 7172-7174; f) O. Schafer, M. Allan, G. Szeimies, M. Sanktjohansert, *J. Am. Chem. Soc.* **1992**,*114*,8180-8186; g) M. Messerschmidt, S. Scheins, L. Grubert, M.l Pätzel, G. Szeimies, C. Paulmann, P. Luger, *Angew. Chem. Int. Ed*. **2005**, *44*, 3925 –3928.

[4] B. Braïda, S. Shaik, W. Wu, P. C. Hiberty, *Chem. Eur. J*. **2020**, *26,* 5935-6939.

[5] S. Kozuch, Org. Lett. **2014**, *16*, 4102−4105.

[6] a) I. Fernandez, G. Frenking, *Chem. Eur. J.* **2006**, *12*, 3617 – 3629; b) G. Gayatri, Y. Soujanya, I. Fernández, G. Frenking, G. Narahari Sastry, *J. Phys. Chem. A* **2008**, *112,* 12919–12924. c) Y. Mo, *Org. Lett*. **2006**, *8*(3), 535-538.

[7] Gaussian 09, Revision A.01, M. J. Frisch, G. W. Trucks, H. B. Schlegel, G. E. Scuseria, M. A. Robb, J. R. Cheeseman, G. Scalmani, V. Barone, B. Mennucci, G. A. Petersson, H. Nakatsuji, M. Caricato, X. Li, H. P. Hratchian, A. F. Izmaylov, J. Bloino, G. Zheng, J. L. Sonnenberg, M. Hada, M. Ehara, K. Toyota, R. Fukuda, J. Hasegawa, M. Ishida, T. Nakajima, Y. Honda, O. Kitao, H. Nakai, T. Vreven, J. A. Montgomery, Jr., J. E. Peralta, F. Ogliaro, M. Bearpark, J. J. Heyd, E. Brothers, K. N. Kudin, V. N. Staroverov, R. Kobayashi, J. Normand, K. Raghavachari, A. Rendell, J. C. Burant, S. S. Iyengar, J. Tomasi, M. Cossi, N. Rega, J. M. Millam, M. Klene, J. E. Knox, J. B. Cross, V. Bakken, C. Adamo, J. Jaramillo, R. Gomperts, R. E. Stratmann, O. Yazyev, A. J. Austin, R. Cammi, C. Pomelli, J. W. Ochterski, R. L. Martin, K. Morokuma, V. G. Zakrzewski, G. A. Voth, P. Salvador, J. J. Dannenberg, S. Dapprich, A. D. Daniels, Ö. Farkas, J. B. Foresman, J. V. Ortiz, J. Cioslowski, D. J. Fox, Gaussian, Inc., Wallingford CT, **2009**

[8] Y. Yamaguchi, B. C. Hoffman, J. C. Stephens, H. F. Schaefer, *J. Phys. Chem. A* **1999**, *103*, 38, 7701–7708

[9] W. A. Shirley, R. Hoffmann, V. S. Mastryukov, *J. Phys. Chem*. **1995**, *99*, 4025.

[10] a) H. A. Bent, J. Chem. Educ. **1960**, *37* (12), 616–624; b) M. J. S. Dewar, H. N. Schmeising, *Tetrahedron* **1959**, *5*, 166-178; c) R. A. Alden, J. Kraut, T. G. Traylor, *J. Am. Chem. Soc.* **1968**, *90*, 74-82; d) S. Osawa, M. Sakai, E. Osawa, *J. Phys. Chem. A* **1997**, *101*, 1378-1383. e) M. G. Brown *Trans. Faraday Soc*., **1959**, *55*, 694-700. f) D. A. Root, C. R. Landis, T. Cleveland, *J. Am. Chem. Soc.* **1993**, *115*, 4201-4209

[11] M. Tanaka, A. Sekiguchi, *Angew. Chem., Int. Ed.* **2005**, *44*, 5821-5823

[12] a) A. Krapp, F. M. Bickelhaupt, G. Frenking, *Chem. Eur. J*. **2006**, *12*, 9196-9216.

[13] P. Vermeeren, W-J. van Zeist, T. A. Hamlin, C. Fonseca Guerra, F. M. Bickelhaupt**,** *Chem. Eur. J*. **2021** doi.org/10.1002/chem.202004653

[14] F.W. Averill, G. S Painter, *Phys. Rev. B* **1986**, *34(4*) 2088-2095

[15] a) F.M.Bickelhaupt, J. K. Nagle, W.L. Klemm, *J. Phys. Chem. A* **2008**, *112,* 2437-2446; b) P. J. Robinson, A.N. Alexandrova, *J. Phys. Chem. A* **2015**, *119*, 12862−12867. c) P. Chaquin, Y. Canac , C. Lepetit, D. Zargarian, R. Chauvin, *Int. J. Quant. Chem*. **2016**, *116*, 1285-1295; d) P. Chaquin, F. Fuster, F. Volatron, *Int. J. Quant. Chem* **2018**, *118*, 25658-25659

[16] T. Tal, J. Katriel, *Theoret. Chim. Acta* **1977**, *46,* 173-181

[17] a) Y. Yamaguchi, R.B. Remington, J.F. Gaw, H. F. Schaefer III, G. Frenking, *Chem. Phys*. **1994**, 180, 55-70; b) Y. Yamaguchi, R.B. Remington, J.F. Gaw, H. F. Schaefer III, G. Frenking, *J. Chem. Phys*. **1993**, *98* (11), 8749-8760; c) Yamaguchi, B. J. DeLeeuw, C. A. Richards, Jr., H. F. Schaefer III, G. Frenking. *J. Am. Chem. Soc.* **1994***, 116,* 11922-11930.

[18] F. Fuster, P. Chaquin, *Int. J. Quant. Chem.* **2019**,*119 (*20), e25996

[19] R. Laplaza, V. Polo, J. Contreras-Garcia, *J. Phys. Chem. A* **2020**, *124*, 176−184

[20] a) K. Exner, P.v. R. Schleyer, *J. Phys. Chem. A* **2001**, *105*, 3407- 3416; b) S. Grimme*, J. Am. Chem. Soc*. **1996**, *118*, 1529-1534

[21] R. Laplaza, C. Cardenas, P. Chaquin, J. Contreras-Garcia, P. W. Ayers, *J. Comp. Chem*. **2020,** *42* (5), 334-343

[22] J. Blanksby, G. B. Ellison, *Acc. Chem. Res.* **2003**, *36,* 4, 255–263

[23] Y. Mo, Org. Lett. **2006**, *8*(3), 535-538.

[24] a) K. W. Wiberg, *Angew. Chem. Int. Ed. Eng*. **1986**, *25*, 312-322; b) K. W. Wiberg, R.A. Fenoglio, *J. Am. Chem. Soc.* **1968**, *90*, 3395-3397.

[25] D.Cremer, J. Gauss, *J. Am. Chem. Soc*. **1986**, *108*, 7467-7477

[26] a) R. D. Bach, O. Dimitrenko, *J. Org. Chem.* **2002**, *67*, 3884-3896; b) R. D. Bach, O. Dimitrenko, *J. Am. Chem. Soc*. **2004** *126*, 4444-4452.

Supplementary data

Si_2H_6 and Ge_2H_6 model. Geometrical parameters R (Å) and bonding energy BE (kcal/mol with respect to two AH_3 in frozen geometry) as functions of θ; opt = 110.4° (Si_2H_6); opt= 110.4° (Ge_2H_6); MP2/cc-pVTZ level of calculation.

Si_2H_6									
θ	140°	130°	120°	opt	100°	90°	80°	70°	60°
R(SiSi)	2.242	2.289	2.321	2.351	2.394	2.492	2.726	3.038	3.287
R(SiH)	1.517	1.497	1.486	1.481	1.477	1.471	1.469	1.483	1.501
BE	83.9	81.8	80.2	76.8	68.8	45.6	15.3	1.1	-0.4
Ge_2H_6									
θ	140°	130°	120°	opt	100°	90°	80°	70°	60°
R(GeGe)	2.271	2.316	2.357	2.398	2.458	2.568	2.800	3.068	3.281
R(GeH)	1.554	1.536	1.525	1.518	1.513	1.505	1.505	1.523	1.546
BE	83.8	81.3	79.0	74.5	65.1	44.1	17.7	6.0	5.7

N_2H_4 in D_{2d} symmetry. Geometrical parameters R (Å) and bonding energy BE (kcal/mol with respect to two NH_2 in frozen geometry) as functions of θ; opt = 119.9°; MP2/cc-pvTZ level of calculation.

N_2H_4 D_{2d}									
θ	150°	130°	opt	110°	100°	90°	80°	70°	60°
R(NN)	1.299	1.326	1.363	1.420	1.507	1.647	1.852	2.054	2.196
R(NH)	1.039	1.008	1.000	0.995	0.993	0.992	0.997	1.008	1.024
BE	166.7	156.63	141.0	119.0	91.0	58.6	31.0	16.3	11.2

Optimized geometries of molecules studied (MP2/cc-pvtz level)

Butadiyne

1	6	0	0.000000	0.000000	0.684335
2	6	0	0.000000	0.000000	-0.684335
3	6	0	0.000000	0.000000	1.903689
4	6	0	0.000000	0.000000	-1.903689
5	1	0	0.000000	0.000000	2.965786
6	1	0	0.000000	0.000000	-2.965786

Tetrahedrylacetylene

1	6	0	0.000000	0.000000	1.365443
2	6	0	0.000000	0.000000	-0.028739
3	6	0	0.000000	0.852836	-1.245152
4	6	0	0.738578	-0.426418	-1.245152
5	6	0	-0.738578	-0.426418	-1.245152
6	1	0	0.000000	1.865724	-1.584871
7	1	0	1.615765	-0.932862	-1.584871
8	1	0	-1.615765	-0.932862	-1.584871
9	6	0	0.000000	0.000000	2.583686
10	1	0	0.000000	0.000000	3.645005

Tetrahedryl-tetrahedrane

1	6	0	0.000000	0.000000	0.709477
2	6	0	-0.000000	-0.000000	-0.709477
3	6	0	0.740741	0.427667	-1.919852
4	6	0	-0.000000	-0.855335	-1.919852
5	6	0	-0.740741	0.427667	-1.919852
6	6	0	0.000000	0.855335	1.919852
7	6	0	0.740741	-0.427667	1.919852
8	6	0	-0.740741	-0.427667	1.919852
9	1	0	1.610621	0.929892	-2.283026
10	1	0	-0.000000	-1.859785	-2.283026
11	1	0	-1.610621	0.929892	-2.283026
12	1	0	0.000000	1.859785	2.283026
13	1	0	1.610621	-0.929892	2.283026
14	1	0	-1.610621	-0.929892	2.283026

Propyne

1	6	0	0.000000	0.000000	-1.243796
2	6	0	0.000000	0.000000	0.214652
3	1	0	0.000000	1.017866	-1.628225
4	1	0	0.881498	-0.508933	-1.628225
5	1	0	-0.881498	-0.508933	-1.628225
6	6	0	0.000000	0.000000	1.428404
7	1	0	0.000000	0.000000	2.489115

Methyl-tetrahedrane

1	6	0	0.000000	0.000000	1.809723
2	6	0	0.000000	0.000000	0.333615
3	6	0	0.000000	0.855953	-0.872305
4	6	0	0.741277	-0.427977	-0.872305
5	6	0	-0.741277	-0.427977	-0.872305
6	1	0	0.000000	1.855820	-1.246812
7	1	0	1.607187	-0.927910	-1.246812
8	1	0	-1.607187	-0.927910	-1.246812
9	1	0	0.000000	-1.019353	2.193965
10	1	0	-0.882786	0.509677	2.193965
11	1	0	0.882786	0.509677	2.193965

Cubyl-cubane

1	6	0	0.000000	0.000000	0.000000
2	6	0	0.000000	0.000000	1.571683
3	6	0	1.564587	0.000000	1.563699
4	6	0	1.571620	-0.001858	-0.000904
5	6	0	1.561805	-1.566438	-0.003751
6	6	0	-0.002810	-1.571615	-0.000960
7	6	0	-0.004724	-1.564601	1.563656
8	6	0	1.560369	-1.565085	1.561350
9	1	0	2.187615	-2.194280	2.189101
10	1	0	2.195543	0.623338	2.193543
11	1	0	-0.629997	-2.193672	2.193462
12	1	0	-0.632916	0.634845	2.189688
13	1	0	2.190536	-2.196997	-0.628610
14	1	0	2.190007	0.631496	-0.634941
15	1	0	-0.637966	-2.188119	-0.635030
16	6	0	-0.844965	0.847669	-0.845468
17	6	0	-0.842083	2.419360	-0.844281
18	6	0	-0.844927	0.847986	-2.417124
19	6	0	-2.416665	0.849702	-0.844613
20	6	0	-2.409524	0.848079	-2.409221
21	6	0	-0.840115	2.412553	-2.408885
22	6	0	-2.406693	2.414307	-0.841568
23	6	0	-2.405207	2.413162	-2.406665
24	1	0	-0.212059	0.213260	-3.035289
25	1	0	-3.035161	0.216330	-0.210713
26	1	0	-3.032426	3.042491	-3.034294
27	1	0	-3.035379	3.044850	-0.216659
28	1	0	-0.214832	3.041733	-3.038567
29	1	0	-0.206921	3.035715	-0.210086
30	1	0	-3.040474	0.224921	-3.039236

Bicyclopentyl-bicyclopentane

1	6	0	0.000000	0.000000	0.000000
2	6	0	0.000000	0.000000	1.476529
3	6	0	1.235875	0.000000	-0.945198
4	6	0	-0.617937	1.070299	-0.945198
5	6	0	-0.617937	-1.070299	-0.945198
6	6	0	0.617937	1.070299	2.421727
7	6	0	0.617937	-1.070299	2.421727
8	6	0	-1.235875	0.000000	2.421727
9	1	0	1.841954	0.905975	-0.940633
10	1	0	1.841954	-0.905975	-0.940633
11	1	0	-0.136379	2.048166	-0.940633
12	1	0	-1.705574	1.142191	-0.940633
13	1	0	-1.705574	-1.142191	-0.940633
14	1	0	-0.136379	-2.048166	-0.940633
15	1	0	0.136379	2.048166	2.417163
16	1	0	1.705574	1.142191	2.417163
17	1	0	1.705574	-1.142191	2.417163
18	1	0	0.136379	-2.048166	2.417163
19	1	0	-1.841954	0.905975	2.417163
20	1	0	-1.841954	-0.905975	2.417163
21	6	0	0.000017	0.000017	-1.878476
22	6	0	-0.000011	-0.000020	3.355005
23	1	0	-0.000025	-0.000043	4.442214
24	1	0	0.000033	0.000038	-2.965685

Butadiene

1	6	0	-0.329758	0.647521	-0.000000
2	6	0	0.329758	-0.647521	-0.000000
3	6	0	0.329758	1.814118	-0.000000
4	6	0	-0.329758	-1.814118	-0.000000
5	1	0	-1.414227	0.645163	-0.000000
6	1	0	1.414227	-0.645163	0.000000
7	1	0	-0.194087	2.758274	-0.000000
8	1	0	0.194087	-2.758274	-0.000000
9	1	0	1.411329	1.839762	-0.000000
10	1	0	-1.411329	-1.839762	-0.000000

Propene

1	6	0	-1.232913	-0.158738	0.000026
2	1	0	-2.015649	0.595245	-0.000171
3	1	0	-1.377883	-0.786249	0.878373
4	1	0	-1.377606	-0.785975	-0.878623
5	6	0	0.136158	0.466050	0.000056
6	6	0	1.275252	-0.228612	-0.000008
7	1	0	0.192737	1.547745	0.000065
8	1	0	2.234189	0.268016	-0.000137
9	1	0	1.273235	-1.310985	0.000047

Toluene

1	6	0	-2.415144	-0.002270	0.000033
2	1	0	-2.809508	-1.016360	0.000061
3	1	0	-2.804712	0.511247	0.878884
4	6	0	-0.912107	-0.006142	-0.000063
5	1	0	-2.805010	0.511537	-0.878477
6	6	0	-0.199887	1.197282	-0.000047
7	6	0	1.192018	1.206440	0.000005
8	6	0	1.898648	0.004672	0.000043
9	6	0	1.202335	-1.200913	0.000010
10	6	0	-0.191752	-1.201943	-0.000057
11	1	0	-0.742565	2.134899	-0.000057
12	1	0	1.724139	2.148118	0.000019
13	1	0	2.979900	0.009033	0.000096
14	1	0	1.741288	-2.138667	0.000022
15	1	0	-0.728201	-2.142563	-0.000091

2,2,3,3-tetramethylbutane

1	6	0	0.000000	0.000000	0.782528
2	6	0	0.000000	0.000000	-0.782528
3	6	0	-1.418321	0.164956	1.337132
4	6	0	0.566304	-1.310780	1.337132
5	6	0	0.852017	1.145824	1.337132
6	6	0	-0.852017	1.145824	-1.337132
7	6	0	1.418321	0.164956	-1.337132
8	6	0	-0.566304	-1.310780	-1.337132
9	1	0	1.815450	1.159684	-1.139447
10	1	0	-0.562430	2.110427	-0.920393
11	1	0	2.108898	-0.568135	-0.920393
12	1	0	1.403062	0.025100	-2.419069
13	1	0	-0.723268	1.202537	-2.419069
14	1	0	-1.912041	0.992384	-1.139447
15	1	0	-0.679794	-1.227637	-2.419069
16	1	0	0.096591	-2.152068	-1.139447
17	1	0	-1.546468	-1.542292	-0.920393
18	1	0	0.723268	1.202537	2.419069
19	1	0	1.912041	0.992384	1.139447
20	1	0	0.562430	2.110427	0.920393
21	1	0	-2.108898	-0.568135	0.920393
22	1	0	-1.403062	0.025100	2.419069
23	1	0	-1.815450	1.159684	1.139447
24	1	0	-0.096591	-2.152068	1.139447
25	1	0	1.546468	-1.542292	0.920393
26	1	0	0.679794	-1.227637	2.419069

Cyclohexane

1	6	0	1.135709	0.904931	0.234992
2	6	0	1.351539	-0.531060	-0.235023
3	6	0	0.215871	-1.435970	0.235046
4	6	0	-1.135653	-0.904953	-0.235030
5	6	0	-1.351569	0.531021	0.235001
6	6	0	-0.215902	1.435983	-0.234971
7	1	0	2.310794	-0.907935	0.122777
8	1	0	1.391821	-0.546973	-1.328254
9	1	0	0.222265	-1.478672	1.328277
10	1	0	0.369094	-2.455198	-0.122635
11	1	0	-1.169452	-0.931908	-1.328262
12	1	0	-1.941698	-1.547264	0.122692
13	1	0	-2.310748	0.907970	-0.122915
14	1	0	-1.392020	0.546846	1.328230
15	1	0	-0.369039	2.455110	0.123009
16	1	0	-0.222352	1.479022	-1.328207
17	1	0	1.169764	0.932036	1.328225
18	1	0	1.941597	1.547257	-0.123020

Methylenecyclopropane

1	6	0	0.000000	0.000000	1.637560
2	6	0	0.000000	0.000000	0.314826
3	6	0	-0.000000	0.769522	-0.930967
4	6	0	-0.000000	-0.769522	-0.930967
5	1	0	-0.000000	0.927484	2.192993
6	1	0	-0.000000	-0.927484	2.192993
7	1	0	-0.912752	1.264168	-1.232173
8	1	0	0.912752	1.264168	-1.232173
9	1	0	0.912752	-1.264168	-1.232173
10	1	0	-0.912752	-1.264168	-1.232173

Cyclopentane

1	6	0	0.775713	-1.027363	-0.072565
2	6	0	1.199241	0.416969	0.216013
3	6	0	0.000454	1.232464	-0.280599
4	6	0	-1.198909	0.417850	0.216070
5	6	0	-0.776509	-1.026785	-0.072642
6	1	0	1.316189	0.572102	1.289968
7	1	0	2.137055	0.689412	-0.264202
8	1	0	0.000449	1.253947	-1.373199
9	1	0	0.000822	2.262668	0.073374
10	1	0	-2.136629	0.691169	-0.263845
11	1	0	-1.315456	0.572858	1.290087
12	1	0	-1.147928	-1.333823	-1.049694
13	1	0	-1.185977	-1.725700	0.654397
14	1	0	1.147130	-1.335104	-1.049397
15	1	0	1.184406	-1.726337	0.654847

Cyclobutene

1	6	0	-0.909002	0.604983	0.002790
2	6	0	-0.496336	-0.884221	-0.021184
3	6	0	0.988341	-0.455433	0.000554
4	6	0	0.599137	0.837360	0.021080
5	1	0	-1.425772	0.508830	0.955495
6	1	0	-0.810247	-1.499500	0.819550
7	1	0	-0.666874	-1.450130	-0.934753
8	1	0	-1.352216	1.011522	-0.903980
9	1	0	1.963360	-0.924442	0.000822
10	1	0	1.198911	1.737583	0.043429

Cyclobutane

1	6	0	0.757332	-0.757538	-0.152879
2	6	0	0.757531	0.757298	0.152889
3	6	0	-0.757304	0.757526	-0.152888
4	6	0	-0.757559	-0.757311	0.152878
5	1	0	0.934441	-0.934560	-1.212866
6	1	0	-1.406096	-1.405694	-0.431553
7	1	0	-0.934720	-0.934278	1.212866
8	1	0	1.405673	-1.406115	0.431555
9	1	0	-1.405671	1.406100	0.431531
10	1	0	0.934686	0.934371	1.212858
11	1	0	1.406090	1.405678	-0.431534
12	1	0	-0.934402	0.934651	-1.212858

Cyclopropane

1	6	0	0.522701	0.522701	0.522701
2	6	0	-0.522701	-0.522701	0.522701
3	6	0	-0.522701	0.522701	-0.522701
4	6	0	0.522701	-0.522701	-0.522701
5	1	0	-1.138859	-1.138859	1.138859
6	1	0	1.138859	-1.138859	-1.138859
7	1	0	1.138859	1.138859	1.138859
8	1	0	-1.138859	1.138859	-1.138859

Cyclopropene

1	6	0	0.000000	-0.000000	0.861579
2	6	0	-0.000000	0.649373	-0.499546
3	6	0	-0.000000	-0.649373	-0.499546
4	1	0	-0.000000	1.578880	-1.035900
5	1	0	-0.000000	-1.578880	-1.035900
6	1	0	-0.912333	0.000000	1.448438
7	1	0	0.912333	-0.000000	1.448438

Tetrahedrane

1	6	0	0.522701	0.522701	0.522701
2	6	0	-0.522701	-0.522701	0.522701
3	6	0	-0.522701	0.522701	-0.522701
4	6	0	0.522701	-0.522701	-0.522701
5	1	0	-1.138859	-1.138859	1.138859
6	1	0	1.138859	-1.138859	-1.138859
7	1	0	1.138859	1.138859	1.138859
8	1	0	-1.138859	1.138859	-1.138859

Bicyclobutane

1	6	0	0.750113	-0.000000	-0.313997
2	6	0	-0.750113	0.000000	-0.313997
3	6	0	-0.000000	1.130771	0.312484
4	6	0	-0.000000	-1.130771	0.312484
5	1	0	-0.000000	1.214060	1.395784
6	1	0	0.000000	2.073678	-0.219140
7	1	0	-0.000000	-1.214060	1.395784
8	1	0	-0.000000	-2.073678	-0.219140
9	1	0	1.401767	-0.000000	-1.167567
10	1	0	-1.401767	0.000000	-1.167567

[1.1.1] Propellane

1	6	0	0.000000	0.000000	0.797800
2	6	0	0.000000	1.290600	0.000000
3	6	0	0.000000	0.000000	-0.797800
4	6	0	-1.117692	-0.645300	0.000000
5	6	0	1.117692	-0.645300	0.000000
6	1	0	0.917248	1.864705	0.000000
7	1	0	-0.917248	1.864705	-0.000000
8	1	0	-1.156257	-1.726713	0.000000
9	1	0	-2.073506	-0.137992	0.000000
10	1	0	2.073506	-0.137992	-0.000000
11	1	0	1.156257	-1.726713	0.000000

Allene

1	6	0	0.000000	-0.000000	0.861579
2	6	0	-0.000000	0.649373	-0.499546
3	6	0	-0.000000	-0.649373	-0.499546
4	1	0	-0.000000	1.578880	-1.035900
5	1	0	-0.000000	-1.578880	-1.035900
6	1	0	-0.912333	0.000000	1.448438
7	1	0	0.912333	-0.000000	1.448438

Benzene

1	6	0	0.000000	1.393655	0.000000
2	6	0	1.206941	0.696827	0.000000
3	6	0	1.206941	-0.696827	0.000000
4	6	0	-0.000000	-1.393655	-0.000000
5	6	0	-1.206941	-0.696827	0.000000
6	6	0	-1.206941	0.696827	0.000000
7	1	0	0.000000	-2.475102	-0.000000
8	1	0	2.143501	-1.237551	-0.000000
9	1	0	-2.143501	-1.237551	-0.000000
10	1	0	2.143501	1.237551	-0.000000
11	1	0	-2.143501	1.237551	-0.000000
12	1	0	0.000000	2.475102	0.000000

Cyclopropenylcyclopropane

1	6	0	0.000000	0.000000	-0.658092
2	6	0	-0.000000	0.000000	0.658122
3	6	0	-0.000000	0.823752	1.846708
4	6	0	-0.000000	-0.823752	1.846708
5	1	0	0.921944	1.143333	2.307577
6	1	0	-0.921944	1.143333	2.307577
7	1	0	-0.921944	-1.143333	2.307577
8	1	0	0.921944	-1.143333	2.307577
9	6	0	0.000000	-0.823752	-1.846678
10	6	0	0.000000	0.823752	-1.846678
11	1	0	-0.921944	-1.143097	-2.307711
12	1	0	0.921944	-1.143097	-2.307711
13	1	0	0.921944	1.143097	-2.307711
14	1	0	-0.921944	1.143097	-2.307711

Ethylene

1	6	0	0.000000	0.000000	0.666024
2	6	0	0.000000	0.000000	-0.666024
3	1	0	0.000000	0.922818	1.227906
4	1	0	-0.000000	-0.922818	1.227906
5	1	0	-0.000000	-0.922818	-1.227906
6	1	0	0.000000	0.922818	-1.227906

Acetylene

1	6	0	0.000000	0.000000	0.605689
2	6	0	0.000000	0.000000	-0.605689
3	1	0	0.000000	0.000000	-1.667231
4	1	0	-0.000000	0.000000	1.667231

Cyclopentyne

1	6	0	1.159043	0.622398	0.000000
2	6	0	-0.185533	1.278265	0.000000
3	6	0	-1.124324	0.000015	0.000000
4	6	0	-0.185533	-1.278236	0.000000
5	6	0	1.159043	-0.622369	0.000000
6	1	0	-0.346237	1.900966	0.878197
7	1	0	-0.346237	1.900966	-0.878197
8	1	0	-0.346237	-1.900936	-0.878197
9	1	0	-0.346237	-1.900936	0.878197
10	1	0	-1.775609	-0.000249	-0.873575
11	1	0	-1.775609	-0.000249	0.873575

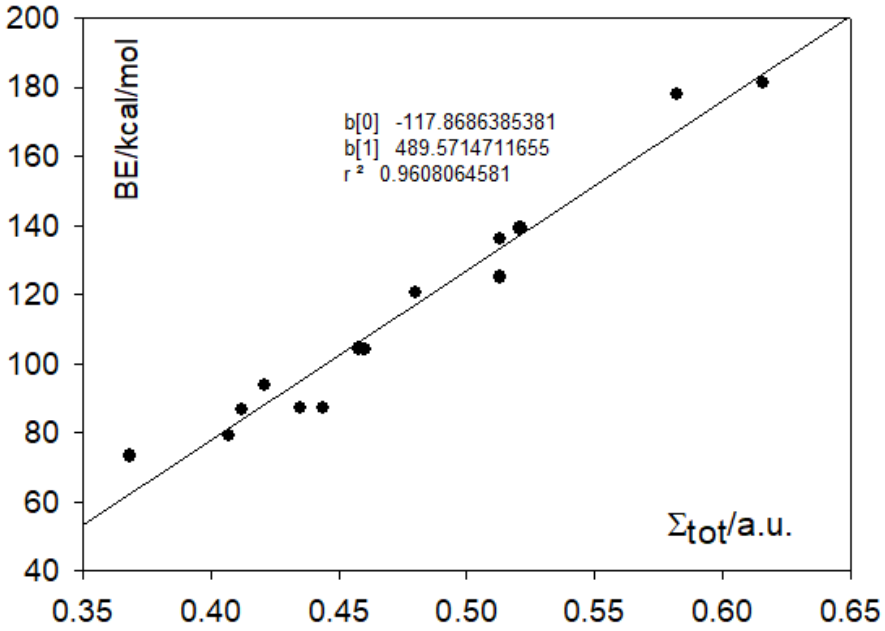

Fig. 1. Correlation between BE (from AIM data, ref 20) and Σ_{tot}